SPANDIDOS PUBLICATIONS

ONCOLOGY LETTERS 20: 179, 2020

Sterically stabilized liposomes targeting P21 (RAC1) activated kinase-1 and secreted phospholipase A_2 suppress prostate cancer growth and metastasis

ARTI VERMA[1,2*], WIDED NAJAHI-MISSAOUI[3*], BRIAN S. CUMMINGS[3,4] and PAYANINGAL R. SOMANATH[1,2,5]

[1]Program in Clinical and Experimental Therapeutics, University of Georgia, Augusta, GA 30912;
[2]Charlie Norwood Veterans Affairs Medical Center, Augusta, GA 30904;
[3]Department of Pharmaceutical and Biomedical Sciences, University of Georgia, Athens, GA 30602;
[4]Interdisciplinary Toxicology Program, University of Georgia;
[5]Department of Medicine and Cancer Center, Augusta University, Augusta, GA 30602, USA

Received May 8, 2020; Accepted July 22, 2020

DOI: 10.3892/ol.2020.12040

Abstract. Metastatic prostate cancer (PCa) has a very high mortality rate in men, in Western countries and lacks reliable treatment. The advanced-stage PCa cells overexpress P21 (RAC1) activated kinase-1 (PAK1) and secreted phospholipase A_2 ($sPLA_2$) suggesting the potential utility of pharmacologically targeting these molecules to treat metastatic PCa. The small molecule, inhibitor targeting PAK1 activation-3 (IPA3) is a highly specific allosteric inhibitor of PAK1; however, it is metabolically unstable once in the plasma thus, limiting its utility as a chemotherapeutic agent. In the present study, the efficacy and specificity of IPA3 were combined with the stability and the $sPLA_2$-targeted delivery method of two sterically stabilized liposomes [sterically stabilized long-circulating liposomes (SSL)-IPA3 and $sPLA_2$ responsive liposomes (SPRL)-IPA3, respectively] to inhibit PCa growth and metastasis. It was found that twice-a-week administration of either SSL-IPA3 or SPRL-IPA3 for 3 weeks effectively suppressed the growth of PC-3 cell tumor xenografts implanted in athymic nude mice. Both drug formulations also inhibited the metastasis of intravenously administered murine RM1 PCa cells to the lungs of C57BL/6 mice. Whereas the twice-a-week administration of SSL-IPA3 significantly inhibited the spontaneous PCa metastasis to the lungs in Transgenic Adenocarcinoma of the Mouse Prostate mice, the administration of free IPA3 had no significant therapeutic benefit. The results present two novel IPA3 encapsulated liposomes to treat metastatic PCa.

Correspondence to: Professor Payaningal R. Somanath, Program in Clinical and Experimental Therapeutics, University of Georgia, HM 102-College of Pharmacy, 914 New Bailie Street, Augusta, GA 30912, USA
E-mail: sshenoy@augusta.edu

*Contributed equally

Key words: P21 (RAC1) activated kinase-1, secreted phospholipase A_2, liposomes, prostate cancer, metastasis

Introduction

Prostate cancer (PCa) ranks second for cancer-related mortality in men, with an expected 33,330 deaths estimated to occur in 2020 worldwide (1,2). Treatment options for the advanced metastatic PCa are limited due to the uncertainties in the molecular mechanisms and the serious side effects of chemotherapy. While the advent of novel screening methods, such as novel serum-based models like 4Kscore® and prostate health index (PHI) (3), and hormone ablation therapies have achieved a ~100% 5-year survival rate for patients with localized PCa, treating patients harboring metastatic PCa, who have a 5-year survival rate of 31%, remains a challenge (4,5). In-depth molecular characterization to detect novel druggable targets, identifying compounds with precise molecular targets and limited off-target effects, and developing novel strategies for drug delivery is critical in improving the 5-year survival rate in patients with metastatic PCa.

Our previous studies and those from other researchers have shown that P21 (RAC1) activated kinase-1 (PAK1) promotes PCa growth and metastasis (6-11) by facilitating cell proliferation, cell survival, motility, invasion, and epithelial-to-mesenchymal transition (11-14). Previous studies have also shown that the small molecule, an inhibitor targeting PAK1 activation-3 (IPA3) was found to be an effective allosteric inhibitor of PAK1, which decreases PCa tumor growth, and metastasis (12-14). However, despite the promising effect of IPA3 on PCa, the compound has limitations related to its pharmacokinetic properties. Specifically, IPA3 is metabolically unstable, therefore, daily administration is required to exert its anti-cancer effects (15), which is not feasible in a clinical setting. Therefore, this limitation was addressed by developing two distinct liposomal formulations of IPA3, one based on the classical sterically stabilized long-circulating liposomes (SSL) (16), and the other, that incorporates lipids, which are selectively targeted by secreted phospholipase A_2 ($sPLA_2$), an

esterase overexpressed in several types of cancer, including PCa (17).

SSL-IPA3 are long-circulating liposomes designed for passive targeting by the enhanced permeability and retention effect (18-20). The base formulation of these SSLs is clinically used for the enhanced delivery of doxorubicin for the treatment of breast cancer (21). The mechanisms of increased efficiency for SSL stems, in part, from the presence of the polyethylene glycol (PEG) coating, which decreases SSL clearance by phagocytes in the reticuloendothelial system, therefore extending their systemic circulation time and alters the pharmacokinetics of the encapsulated drug (22). The efficacy of SSL for the treatment of cancer is further enhanced due to the leaky vasculature of tumors and the lack of a functional lymphatic system, which provides access for SSL to enter and accumulate in the tumors by the enhanced permeability and retention phenomenon (23-26). Besides, this also provides passive targeting of SSL to the tumors, as the intact vasculature in normal tissue limits the entry of SSL, decreasing off-target toxicity (27-29). $sPLA_2$ responsive liposomes, or SPRL, are the base formulation of SSL with alterations that include an increase in the negatively charged glycerophospholipids (22). These alterations ensure that SPRL is more responsive to cancers, that overexpress $SPLA_2$, including prostate, breast, gastric, lung, and colon cancers (30,31). $sPLA_2$ cleave phospholipids at the *sn-2* (a nucleophilic substitution in which the rate-determining step involves 2 components) bond of the glycerol backbone releasing fatty acid and lysophospholipids (31-35). Unlike other PLA_2, $sPLA_2$ has a strong affinity for negatively charged phospholipid head groups, in particular, phosphatidylserine, phosphatidylglycerol, and phosphatidylethanolamine (17,36). In PCa, $sPLA_2$ overexpression was associated with poor clinical prognosis and 5-year survival rate, and the levels of $sPLA_2$ in PCa tissues were reportedly 10-20-fold higher compared with that in normal tissue (31,37-39). Our previous studies demonstrated the increased ability of SPRL, which contained doxorubicin, to decrease PCa growth in a mouse xenograft model (19) and validated its use as a targeted drug delivery system (17,19). SPRL increased their affinity to bind to the cell surface-expressed $sPLA_2$ on the tumor cells, due to the higher concentrations of phosphatidylethanolamine (PE) in their formulation (22,31,36,37).

Despite our previous success with SPRL, it has only been tested in non-metastatic cancer models and has only been formulated with doxorubicin, a drug that is not commonly used for the treatment of PCa (19). Therefore, in the present study, IPA3-encapsulated SSL and SPRL (SSL-IPA3 and SPRL-IPA3, respectively) were created and their efficacies in inhibiting the growth of PCa xenografts and PCa metastasis to the lungs was investigated. The results showed that both SSL and SPRL had increased efficacy compared with that in free IPA3, in the treatment of the tumors, which only required twice-weekly IP injections, as opposed to daily use.

Materials and methods

Cell culture. The human PC-3 (CRL-1435) and murine RM-1 (CRL-3310) metastatic PCa cells were purchased from ATCC. Cells were grown in either DMEM high-glucose medium (for PC-3 cells) or RPMI 1640 medium (for RM-1 cells) (Hyclone; GE Healthcare Life Sciences), supplemented with 10% FBS (R&D Systems, Inc.), 100 U/ml penicillin, and 100 mg/ml streptomycin (Themo Fisher Scientific, Inc.) at 37˚C in a humidified incubator with 5% CO_2. Cells were passaged when they were 80-90% confluent. All the other analytical reagents were purchased from Thermo Fisher Scientific, Inc. unless otherwise stated.

Animals. All the animal procedures were performed according to the protocol approved by the Institutional Animal Care and Use Committee at the Charlie Norwood Veterans Affairs Medical Center, (GA, USA; protocol no. 19-04-114). The protocols were also in agreement with the Animal Research: Reporting of *in vivo* Experiments (ARRIVE) guidelines (40). Briefly, animals were housed 2-4 mice per cage, in rooms maintained at 65-75˚F (~18-23˚C), 40-60% humidity, a 10/14-h light/dark cycle, and *ad libitum* access to food and water. Animals were handled as minimally as possible, with minimal noise levels to avoid any stress. Athymic nude mice (Harlan Laboratories, Inc.) were maintained in sterile cages (2 mice per cage) in a separate sterile room, with the provision of sterile food and water. Isoflurane (3-4% in oxygen) was used to anesthetize mice at the end of the experiment, before euthanasia by cervical dislocation. A total of 90 male 8-10 week-old mice weighing between 25-29 g were used for the tumor and metastasis experiments, with 6 to 11 mice per experiment. Mice were monitored every day for any potential infections or sickness and weighed every 2nd day to determine any weight loss beyond 20%. No animals died before the end of the experiment.

Preparation of liposomal encapsulated IPA3. SSL-IPA3 liposomes were prepared as described in our previous study (16), using the thin lipid hydration method followed by freeze-thaw cycles and a high-pressure extrusion (19,22). Briefly, cholesterol (5 μmol/ml), phospholipids, including 1,2-distearoyl-*sn*-glycero-3-phosphocholine (DSPC) (9 μmol/m) and DSPE-PEG (1 μmol/ml) in chloroform, and IPA3 (4 μmol/ml) in ethanol were added into a round bottom flask. SPRL-IPA3 was also prepared similarly using 5 μmol/ml cholesterol, 8 μmol/ml DSPC, 1 μmol/ml 1,2-distearoyl-*sn*-glycero-3-phosphoethanolamine-N-[poly(ethylene glycol) 2000] (DSPE-PEG), 1 μmol/ml DSPE (17). The solvents were evaporated under vacuum in a water bath at 65˚C using a rotary evaporator (Buchi Labortechnik AG). The formed thin film was then hydrated and suspended in PBS to achieve a final lipid concentration of 10 μmol/ml. The formulation then underwent five liquid nitrogen freeze-thaw cycles, above the phase transition temperature of the primary lipid, before passing five times through a Lipex Extruder (Northern Lipids, Inc.) at 65˚C using double-stacked polycarbonate membranes (80-nm; Suez Water Technologies and Solutions). Excess unencapsulated IPA3 and lipids were eliminated using dialysis in 10% (w/v) sucrose for at least 20 h, with three changes of the dialysis media. Liposome suspensions were stored at 4˚C, protected from light, and used within 24-48 h of preparation. Empty SPRL was also formulated and used as vehicle controls. Quantification of IPA3 was evaluated using methods previously described (16). The quality control

used during the formulation of SSL and SPRL included the measurement of size, zeta potential, and drug encapsulation. The size was measured by both dynamic light scattering and by tandem electron microscopy. Liposomes that did not meet the minimum required characteristics of 1,000 μM IPA3 encapsulation, a size of 100 nm hydrodynamic diameter, a poly-dispersity index of <0.3, and charge of at least-20 mV zeta potential were not used for the experiments.

Mouse genotyping. For the genotyping of Transgenic Adenocarcinoma of the Mouse Prostate (TRAMP) mice (Jackson Laboratory), DNA was extracted from the ear punch of 10 to 21-day old litters. Tissues were incubated with 50 μl of alkaline lysis buffer containing 25 ml H_2O, 62.5 μl of 10 N NaOH, and 10 μl of 0.5 M disodium EDTA at 95˚C for 90 min, followed by neutralization with 50 μl buffer containing 24 ml H_2O, 1 ml 1 M Tris-HCl (41). The TRAMP transgene (600 bp) was amplified using the following primer sequences: Forward 5'-GCGCTGCTGACTTTCTAAACATAAG-3' and reverse, 5'-GAGCTCACGTTAAGTTTTGATGTGT-3', with an annealing temperature of 55˚C. GAPDH was measured as an internal positive control using the following primer seuqneces: Forward, 5'-CTAGGCCACAGAATTGAAAGATCT-3' and reverse, 5'-GTAGGTGGAAATTCAGCATCATCC-3'. PCR was performed using the GoTaq® M712C green master mix (Promega Corporation) with the following thermocycling conditions: Step-1: 95˚C for 3 min; Step-2: 94˚C for 30 sec; Step-3: 60˚C for 1 min; Step-4: 72˚C for 1 min (step-2-4 repeated for 35 cycles); Step-5: 72˚C for 2 min and Step-6: Hold at 4˚C until further processing. The products were visualized using ethidium bromide containing agarose gel (2%) under UV light.

Cell proliferation assay. Cell proliferation following IPA3 treatment was assessed using an MTT assay (Thermo Fisher Scientific, Inc.), as previously described (13). Briefly, cells were seeded into 48-well cell culture plates, at a density of $5x10^4$ cells/ml per well and incubated at 37˚C in a humidified incubator with 5% CO_2 for 24 h. Cells were treated with either 10, 20, or 30 μM IPA3 (cat. no. 3622; Tocris BioScience) encapsulated in SSL and SPRL liposomes, empty SSL and SPRL or dimethyl sulfoxide (DMSO) (vehicle) as controls for 24 h. Following this, MTT reagent was added, at a final concentration of 0.25 mg/ml, and the plates were incubated at 37˚C for 2 h. After incubation, non-reduced MTT and the medium were aspirated and MTT formazan crystals were dissolved using DMSO. Following an additional 15 min incubation, with constant shaking ($2.8x10^{-3}$ x g using a Vari-Mix Platform Rocker (Thermo Fisher Scientific, Inc.), plates were read at 590 nm using a Biotek plate reader (Agilent Technologies, Inc.).

In vivo prostate tumor xenograft assay. PC-3 cells were grown to 60-70% confluent in T75 flasks. Next, the cells were collected and suspended in sterile normal saline. Cell suspension ($3x10^6$ cells/100 μl) was subcutaneously injected into the right flank of 6 to 8-week-old male athymic nude mice (Harlan Laboratories, Inc.). All treatments (empty liposomes, SSL-IPA3, and SPRL-IPA3 (5 mg/kg) were started on day 3 from tumor implantation and were administered two times a week, by intraperitoneal (i.p.) injection. Tumor diameters were measured using digital calipers on days 7, 14, 19, and 21, and the tumor volume (mm^3) was calculated by the modified ellipsoidal formula (tumor volume=½ [length x width^2]). The average size of the tumors before treatment was 42 mm^3. Mice were sacrificed on day 25 and tumors were dissected, weighed, and snap-frozen for further analysis. We included 12 mice in each group at the start of the experiment. However, one mouse from the empty liposome group, one from the SSL-IPA3 group and two mice from the SPRL-IPA3 group were later removed due to sickness.

In vivo mouse lung colonization (metastasis) assay. PC-3 and RM-1 cells grown to 60-70% confluence in T75 flasks were washed once with 1X PBS, detached using trypsin, and re-suspended in 0.9% saline. A total volume of 150 μl cell suspension, containing $0.5x10^6$ cells was injected through the tail-vein into 8-week-old C57BL/6 mice, as well as athymic nude mice. Animals in each group were injected (i.p.) with either 5 mg/kg SSL-IPA3 or SPRL-IPA3, or vehicle control (PBS or empty liposomes) twice weekly as previously described (18). Alternately, 27-week old TRAMP mice were injected with the vehicle (sterile PBS), free IPA3 twice a week, free IPA3 once daily, or SSL-IPA3 twice a week for 3 weeks. Mice weight was monitored every 3 days, up to day 21. On day 21, mice were euthanized, the lungs were collected and snap-frozen or directly fixed for hematoxylin and eosin (H&E) staining. The number of lung nodules was counted by three blinded reviewers (individuals within the laboratory) and the average of their scores was used for analysis. In the TRAMP mice study, 8 mice were included in each at the start of the experiment. However, one mouse from the twice-weekly free IPA3 group and two mice from the once per day free IPA3 group were removed due to sickness.

Histological examination of the mouse lungs. Tissue sections were embedded in paraffin and 5 μm sections were cut for H&E staining. For staining, tissues were first dehydrated twice with 95% ethanol for 30 min each, followed by soaking in xylene for 1 h at 60-70˚C. The sections were subsequently dipped in paraffin for 12 h. Tissue sections were stained with Harris' hematoxylin solution for 6 h at 60-70˚C, rinsed in tap water and immersed in a destaining solution containing 10% acetic acid and 85% ethanol in water for 2 h and an additional 10 h at room temparature. Washing slides were soaked in a saturated lithium carbonate solution for 12 h and rinsed with tap water. Finally, sections were stained with eosin Y in ethanol for 48 h at room temparature. Imaging was performed using a brightfield Keyence BZ-X800 microscope (Keyence Corporation; magnification, x4). Lung micrometastasis was analyzed using ImageJ software (version 1.48v; National Institutes of Health) (13). Briefly, the H&E images of the lung were converted to grayscale followed by splitting the image into RGB channels. The area of individual channels was measured and subtracted from the total lung area to determine the metastatic area.

Statistical analysis. Data are presented as the mean ± SD. The 'n' value for each figure indicates the number of samples in each group. MTT assays were performed 6 times in 3 replicates. All

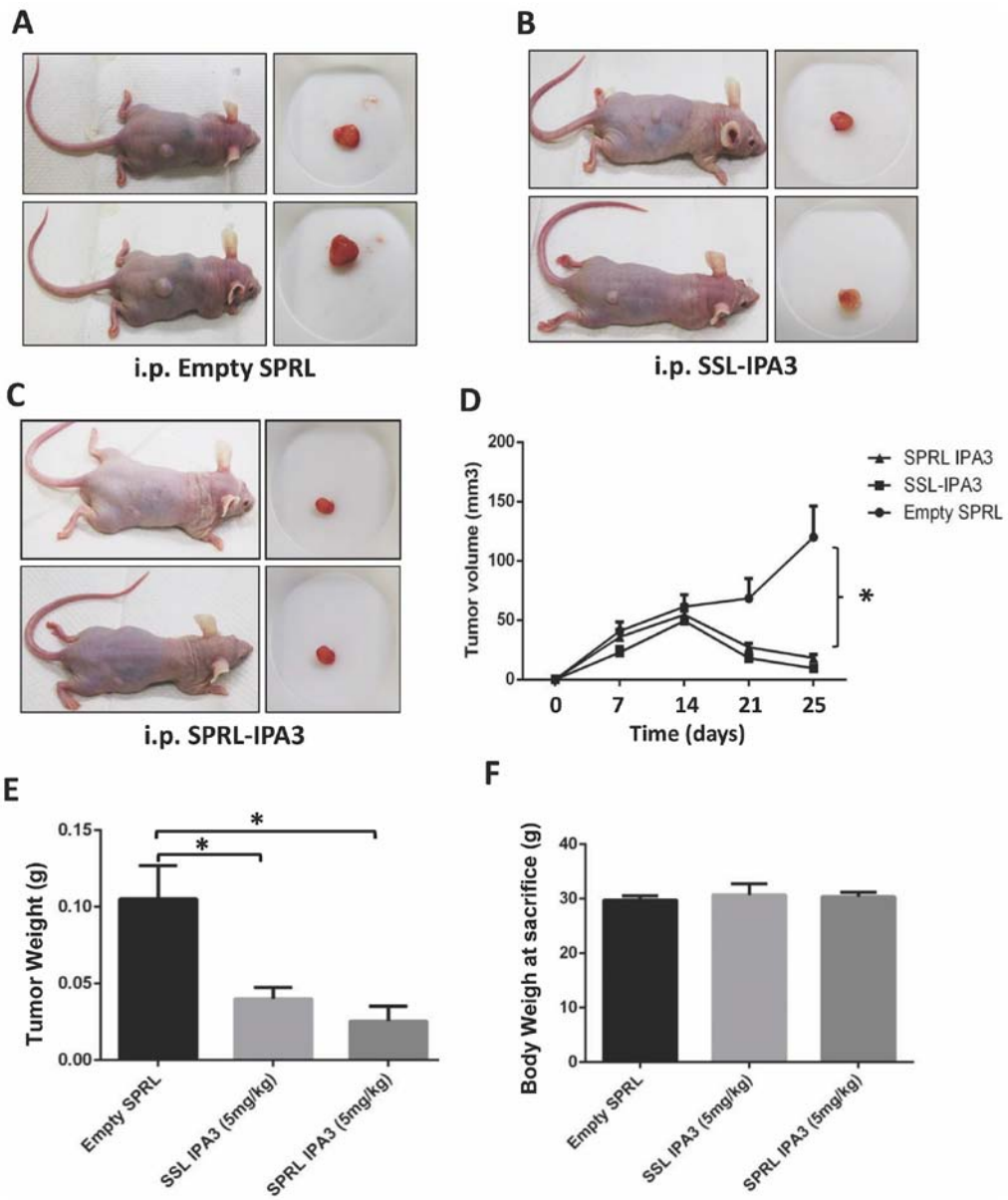

Figure 1. SSL-IPA3 and SPRL IPA3 significantly inhibits the growth of PC-3 cell tumor xenografts in athymic nude mice. Images of athymic nude mice bearing PC-3 cell tumor xenografts (left) and extracted tumors (right) treated with (A) empty liposomes, (B) SSL-IPA3, and (C) SPRL-IPA3 (5 mg/kg). (D) Line graph showing the volume of PC-3 cell tumor xenografts on days 7, 14, 21 and 25, following implantation in athymic nude mice treated with empty liposomes, SSL-IPA3 and SPRL-IPA3 (5 mg/kg), respectively. Bar graph showing the (E) weight of the tumors and (F) body weight of PC-3 cell tumor xenograft athymic nude mice treated with empty liposomes, SSL-IPA3 and SPRL-IPA3 (5 mg/kg), respectively on day 25 post-tumor implantation. Data are presented as the mean ± SD. One-way ANOVA was used to compare when there were more than two groups. *P<0.001. i.p., intraperitoneal; SRPL, secreted phospholipase A_2 responsive liposomes; SSL, sterically stabilized long-circulating liposomes; IPA3, P21 (RAC1) activated kinase-1. Empty liposomes (n=11), SSL-IPA3 group (n=11), SPRL-IPA3 group (n=10).

the data were analyzed using parametric tests, the Student's unpaired t-test for comparing two groups or one-way ANOVA for comparing more than two groups, followed by Tukey's post hoc test (with pooled variance) and the GraphPad Prism v6.01 software (GraphPad, Software, Inc.) P<0.05 was considered to indicate a statistically significant difference.

Results

SSL-IPA3 and SPRL-IPA3 suppress the growth of PC-3 cell tumor xenografts in athymic nude mice with similar efficacy. Our previous study found that SSL-IPA3 was more effective in decreasing PC-3 tumor xenograft growth compared with that for free IPA3 (16); however, the ability of SPRL-IPA3 to decrease tumor growth in xenograft models has never been investigated. Twice-weekly administration of SSL-IPA3 (5 mg/kg) inhibited the growth of PC-3 tumor xenografts compared with that in the control group (Fig. 1A-C). Furthermore, the same results were demonstrated with SPRL-IPA3, administrated at the same dose and schedule (Fig. 1A-C). The results were found to be significantly different for tumor volume (Fig. 1D) and weight (Fig. 1E). There was no significant difference between empty liposomes, SSL-IPA3, and SPRL-IPA3 treatment on the total body weight of mice after 25 days (Fig. 1F). The data revealed that SSL-IPA3 and SPRL-IPA3 are effective in inhibiting the growth of prostate tumor xenografts.

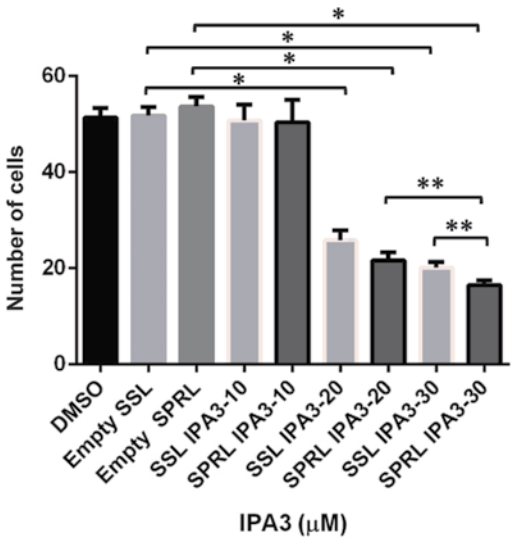

Figure 2. SSL-IPA3 and SPRL-IPA3 significantly inhibit RM-1 murine metastatic PCa cell proliferation *in vitro*. A bar graph representing a dose-dependent reduction in cell proliferation following 24 h treatment with SSL-IPA3 and SPRL-IPA3 (5 mg/kg) in RM-1 cells compared with that in cells treated the vehicle (DMSO) and respective empty liposome-treated controls (n=6). Data are presented as the mean + SD. One-way ANOVA was used to compare when there were more than two groups. *P<0.001 and **P<0.01. DMSO, dimethyl sulfoxide; SRPL, secreted phospholipase A_2 responsive liposomes; SSL, sterically stabilized long-circulating liposomes; IPA3, P21 (RAC1) activated kinase-1.

SSL-IPA3 and SPRL-IPA3 inhibit murine RM-1 PCa cell proliferation in vitro. The lung metastasis model used in the present study required mouse PCa cells; however, to the best of our knowledge the effect of SSL- or SPRL-IPA3 to inhibit mouse prostate cell growth has not been previously investigated. Therefore, the effect of this formulation on murine prostate RM-1 metastatic PCa cell proliferation *in vitro* was performed using the MTT assay. It was found that 20 and 30 μM doses for both SSL- and SPRL-IPA3 decreased the number of cells compared with that in cells treated with 10 μM after 24 h (Fig. 2). There was a significant decrease in cell proliferation with 30 μM SRPL-IPA3 compared with that in cells treated with 20 μM SPRL-IPA3, but not between 20 and 30 μM SSL-IPA3. There was also a modest but significant reduction in RM-1 cell proliferation in cells treated with 30 μM SPRL-IPA3 compared with that in cells treated with 30 μM SSL-IPA3. These data suggested that both SSL- and SPRL-IPA3 have antiproliferative effects on RM-1 cells.

SSL-IPA3 and SPRL-IPA3 inhibit RM-1 cell metastasis to the lungs of mice. To the best of our knowledge, liposomal encapsulated IPA3, in any formulation, has never been investigated for its ability to inhibit cancer metastasis. Therefore, the effect of twice-weekly administration of SSL-IPA3 and SPRL-IPA3 on lung metastasis in C57BL/6 mice, following their intravenous injection with RM-1 cells, was determined. Histological examination of the mouse lungs demonstrated a significant reduction in lung metastasis, as measured by the number of colonies and areas of lung metastasis indicated by red arrows with intravenous RM-1 cell injection compared with that in the vehicle group (Fig. 3A). Both SSL-IPA3 and SPRL-IPA3 (5 mg/kg) significantly reduced the number of lung nodules and metastatic areas in the mouse lungs compared with that in the empty liposomes or vehicle control (PBS) groups (Fig. 3B and C). SSL-IPA3 and SPRL-IPA3 were found to be equally effective in inhibiting PCa cell lung metastasis in mice.

Twice-weekly administered SSL-IPA3 but not free IPA3 inhibited lung metastasis in TRAMP mice. To further investigate the ability of SSL- and SPRL-IPA3 to prevent metastasis the effect of twice-weekly injected liposomal IPA3 was compared with that in free IPA3, to inhibit spontaneous lung metastasis, that occurs in TRAMP mice. This mouse model closely resembles the pathogenesis of human PCa and is known to spontaneously develop metastasis at the age of 28-30 weeks (41). TRAMP mice, at 27 weeks of age were injected twice a week with a vehicle (sterile PBS) or free IPA3, or once daily with free IPA3, or twice a week with SSL-IPA3 for 3 weeks (until 30 weeks of age). SPRL-IPA3 was not investigated, as both SSL-IPA3 and SPRL-IPA3 were both efficacious at reducing tumor growth in the aforementioned experiments. Spontaneous lung metastasis in the TRAMP (control and treated) mice were examined using H&E staining of lung sections (Fig. 4A), following 3 weeks of treatments. Histological examination of the lung sections revealed lung metastatic nodules in vehicle-treated TRAMP mice. The area of metastatic nodules was markedly lower in TRAMP mice, administered daily with free IPA3. Notably, twice-weekly treatment with free IPA3 (5 mg/kg) in TRAMP mice did not inhibit PCa lung metastasis in TRAMP mice (Fig. 4A and B). As expected, SSL-IPA3 (5 mg/kg) administration, twice per week for 3 weeks significantly inhibited PCa lung metastasis in TRAMP mice (Fig. 4A and B). These results indicated that the administration of liposome-encapsulated IPA3 twice weekly for 3 weeks could significantly decrease lung metastasis *in vivo* and could be developed into a future therapeutic approach to treat metastatic PCa in humans.

Discussion

Despite the FDA approval of three new drugs, abiraterone acetate, enzalutamide, and radium-223, for front-line use in men with metastatic castration-resistant PCa in the past 5 years, the life expectancy for patients with PCa, over the past decade has only been prolonged by one year (42,43). As a result, patients with metastatic PCa can succumb to the disease, which accounts for the second leading cause of cancer-associated death in men in the US as of 2020 (1,2). Thus, there is an urgent requirement for novel and effective therapeutic strategies for the treatment of metastatic PCa. The higher expression level of PAK1 protein has been found in human PCa tissues and PCa metastasized lung lesions in patients compared with that in the normal tissues from healthy controls (9). Our previous studies have demonstrated that PAK1 was essential for PCa growth, epithelial-to-mesenchymal transition and metastasis, and that the PAK1 allosteric inhibitor, IPA3, was a potential drug to treat metastatic PCa (6,8-10,12,13,16). These findings suggested that PAK1 could be a potential therapeutic target to prevent PCa growth and metastasis in humans.

Several PAK inhibitors have been studied for their anti-cancer efficacies *in vitro* and *in vivo* (10,14,15,44,45). Several PAK1 inhibitors, such as G-5555 (46), FL172 (47), PF-3758309 (48), and AZ13705339 (49) have demonstrated

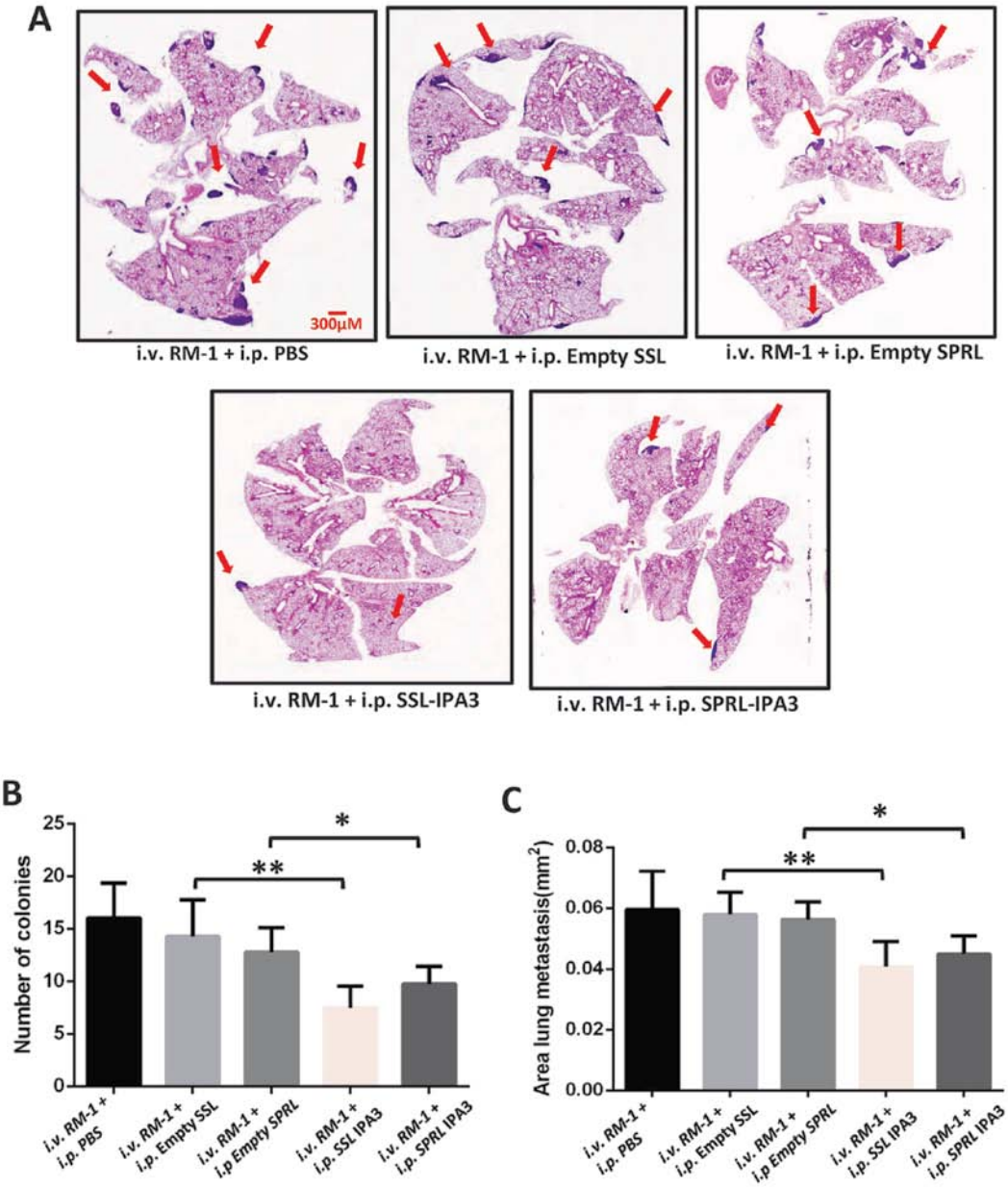

Figure 3. SSL-IPA3 and SPRL-IPA3 significantly inhibit lung metastasis of intravenously administered RM-1 cells in C57BL/6 mice. (A) Representative H&E-stained lung section images showing a marked decrease in lung colonization of RM-1 cells, 21 days following injection with SSL-IPA3, and SPRL-IPA3 (5 mg/kg) compared with that in the control and empty SSL and SPRL liposome-treated groups (n=6). The red arrows indicate the areas of colonization. Bar graphs showing a significant reduction in the (B) number of nodules and (C) area of lung colonization on day 21 following treatment with SSL-IPA3 and SPRL-IPA3 (5 mg/kg) compared with that in the control and empty SSL and SPRL groups. (n=6). Data are presented as the mean ± SD. An unpaired Student's t-test was used to compare between two groups and one-way ANOVA was used to compare among all the groups. *P<0.05; **P<0.01. *i.p.*, intraperitoneal; *i.v.*, intravenous; SRPL, secreted phospholipase A_2 responsive liposomes; SSL, sterically stabilized long-circulating liposomes; IPA3, P21 (RAC1) activated kinase-1; PBS, control group.

PAK1 activity suppression *in vitro*; however, these compounds also exhibited off-target effects on several other kinases, such as the Src family of kinases, Akt1, AMP Kinases, Cyclin-dependent kinase-7 and serum glucocorticoid kinase, due to their competition for the ATP-binding site, that is conserved in several kinases (44,45). Among these, PF-3758309 and PF-03758309 are specific inhibitors of PAK4, a group II PAK isoform (50), and a clinical trial on PF-03758309 for advanced solid tumors (NCT00932126) was terminated, due to the undesirable pharmacokinetic characteristics, such as unfavorable levels of the drug in the plasma and the lack of a dose-response association. Therefore, the allosteric PAK1 inhibitors, such as IPA3 (15) and NVS-PAK1-1 (51) were preferred for pharmacological interventions in cancer research. Our previous studies have demonstrated that IPA3, suppresses epithelial-to-mesenchymal transition, and micro-invasion of PCa cells *in vitro* and tumor growth *in vivo* (6,9). Daily administration of IPA3 also attenuated PCa-induced metastasis and bone remodeling in athymic nude mice (13). Unfortunately, IPA3 in its free form can be rapidly metabolized in the plasma and has a very short half-life (45), which limits its use as a therapeutic agent for cancer. Therefore, it is not feasible to treat patients with cancer in the clinic daily. To overcome this, two new liposome formulations were utilized, with distinct lipid

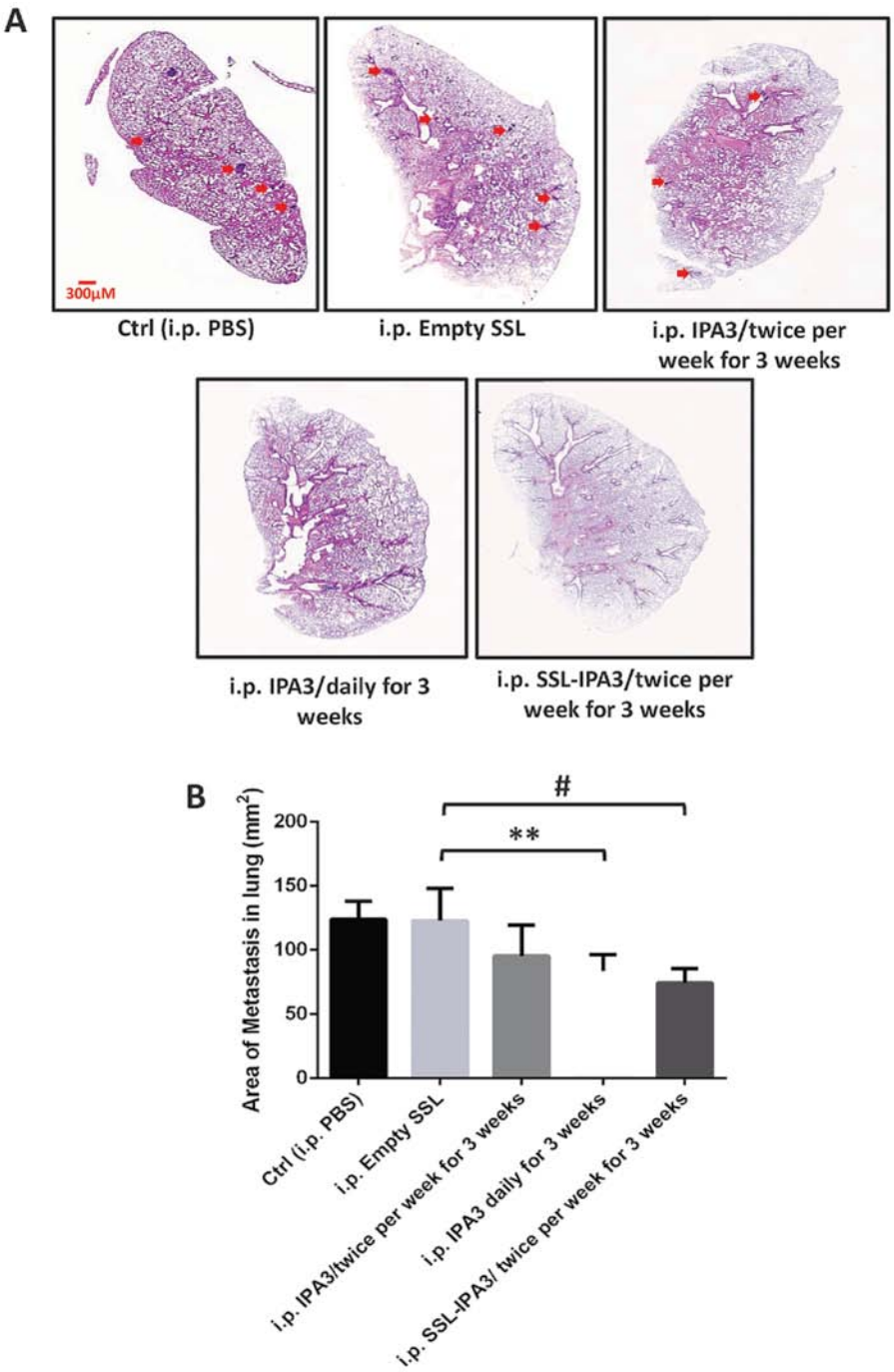

Figure 4. SSL-IPA3 inhibits lung metastasis in TRAMP mice. TRAMP mice, at 27 weeks of age were injected with vehicle, empty SSL, and SSL-IPA3 (5 mg/kg) twice weekly and compared with free IPA3 administered daily or twice weekly for 3 weeks, for lung colonization. (A) Images of H&E-stained TRAMP lung sections showing changes in lung metastasis between the control, free IPA3, and SSL-IPA3-treated groups for 3 weeks. The arrows indicate the area of metastasis. (B) Bar graph indicating reduced lung metastasis in daily administered free IPA3 and twice-weekly administered SSL-IPA3 groups compared with that in the control groups and twice-weekly administered free IPA3 group. Data are presented as the mean ± SD. An unpaired Student's t-test was used to compare between two groups and one-way ANOVA for more than two groups. **P<0.01; $^{\#}$P<0.001. TRAMP, Transgenic Adenocarcinoma of the Mouse Prostate; PBS, vehicle group; i.p., intraperitoneal; SRPL, secreted phospholipase A_2 responsive liposomes; SSL, sterically stabilized long-circulating liposomes; IPA3, P21 (RAC1) activated kinase-1; Ctrl, control. Control, Empty SSL (n=8), twice-weekly administered free IPA3 (n=7), daily administered free IPA3 for 3 weeks (n=6), twice-weekly administered SSL-IPA3 for 3 weeks (n=8).

composition to encapsulate IPA3 into nanoliposomes to serve as a reservoir for its slow release thus, increasing the half-life of the drug in the plasma. Due to the different lipid composition, while both SSL-IPA3 and SPRL-IPA3 have the benefit of high stability and long half-life once in the blood, SPRL-IPA3 has the specificity to respond to the highly expressed $sPLA_2$ in the tumor microenvironment (12,17,36).

In the present study, loading IPA3 into nanoliposomes reduced the frequency of drug administration without compromising its efficacy. The efficacy of SSL-IPA3 or SPRL-IPA3, when administered twice a week, was comparable to the efficacy of daily administration of free IPA3 in preventing PCa lung metastasis in 2 different mouse models. A total of 30 μM SPRL-IPA3 exhibited slightly higher efficacy on

reducing cell survival compared with that in cells treated with a similar dose of SSL-IPA3; however, the efficacies of either of IPA3-containing liposomes were similar even in inhibiting the growth of human PCa tumor xenografts implanted in immunocompromised mice. This frequency of drug administration was not effective with the free form of IPA3 to prevent PCa growth, as evidenced in our previous study (16). The advantage of liposomal IPA3 was also clear from the observation that twice a week administration of free IPA3 did not prevent PCa metastasis to the mouse lungs thus, presenting the liposomal-IPA3 approach as a reliable method to treat metastatic PCa.

Several laboratories have utilized nanoparticles for targeted drug delivery in various types of cancer, including breast, lung, colon, and gastric cancers, which is similar to our approach, where these nanoparticles were enriched in tumors thus, delivering small molecule inhibitors specifically at the tumor site (52-56). To the best of our knowledge, these data are the first to demonstrate the ability of liposomal formulations of IPA3 to inhibit the lung metastasis of PCa. This was observed in two different models of PCa metastasis, representing two different strains of mice, which supports the rigor of our findings. Since PAK1 hyperactivation has also been reported in other diseases, such as osteoarthritis (57), neurodevelopmental disorders (58), macrocephaly (59), intellectual disability (60), and kidney injury (61), liposomal IPA3 could have potential therapeutic applications for several non-cancer human diseases.

The results from the present study show that the efficacies of SSL-IPA3 and SPRL-IPA3 were very similar. The exact reason for this is currently unknown, and requires further investigation; however, it could be due to the specific advantage of each of these formulations; SSL was highly stable and long-acting, while SPRL had additional specificity in targeting the tumor tissues. Another possibility is that both liposomes release their contents before reaching the tumor tissue, but are still able to maintain a constant level of IPA3 in the plasma. Furthermore, a previous study demonstrated the increased efficacy of SPRL over SSL using doxorubicin as the payload (19). This suggested that the differential efficacy of these liposomes may be drug-dependent. It is also important to note that SPRL was designed and validated against human Group IIA $sPLA_2$, as opposed to the mouse $sPLA_2$ isoform. Thus, a potential difference in the activity of group IIA $sPLA_2$ in mice compared with humans may have accounted for SPRL-IPA3 not having a superior efficacy over SSL-IPA3. Additional investigations are required to validate this hypothesis. However, these data still provide strong evidence that PCa growth and metastasis could be targeted effectively by the encapsulation of IPA3, in two different lipid-based nanoparticles. This treatment strategy would allow for the administration of the drug less frequently and improve drug efficacy while minimizing its side-effects.

Acknowledgements

Not applicable.

Funding

The work was primarily funded by the Department of Defense Prostate Cancer Research Program Idea Development Award (grant no. PC150431 GRANT11996600). Partial financial support was also provided by the National Heart Lung and Blood Institute (grant no. R01HL103952), National Center for Advancing Translational Sciences (grant no. UL1TR002378), Wilson Pharmacy Foundation (intramural), and Translational Research Initiative grant (intramural). This work has been accomplished using the resources and facilities at the VA Medical Center in Augusta, GA (USA).

Availability of data and materials

The datasets used and/or analyzed during the present study are available from the corresponding author upon reasonable request.

Author's contributions

AV, WNM, BSC, and PRS contributed to the design and conception of the study and acquired, analyzed, and/or interpreted the data. AV, BSC, WNM, and PRS drafted the initial manuscript. All authors approved the final version of the manuscript.

Ethics approval and consent to participate

Ethics approval was granted by the Institutional Animal Care and Use Committee at the Charlie Norwood Veterans Affairs Medical Center (Georgia, USA; approval no. ACORP #19-04-114).

Patient consent for publication

Not applicable.

Competing interests

The authors declare that they have no competing interests.

References

1. American Cancer Society. Cancer Facts and Figures 2020. Atlanta, American Cancer Society.
2. Siegel RL, Miller KD and Jemal A: Cancer statistics, 2020. CA Cancer J Clin 70: 7-30, 2020.
3. Tan GH, Nason G, Ajib K, Woon DT, Herrera-Caceres J, Alhunaidi O and Perlis N: Smarter screening for prostate cancer. World J Urol 37: 991-999, 2019.
4. Siegel RL, Miller KD and Jemal A: Cancer statistics, 2019. CA Cancer J Clin 69: 7-34, 2019.
5. Malvezzi M, Carioli G, Bertuccio P, Boffetta P, Levi F, La Vecchia C and Negri E: European cancer mortality predictions for the year 2018 with focus on colorectal cancer. Ann Oncol 29: 1016-1022, 2018.
6. Al-Azayzih A, Gao F and Somanath PR: P21 activated kinase-1 mediates transforming growth factor β1-induced prostate cancer cell epithelial to mesenchymal transition. Biochim Biophys Acta 1853: 1229-1239, 2015.
7. Al-Maghrabi J, Emam E, Gomaa W, Al-Qaydy D, Al-Maghrabi B, Buhmeida A, Abuzenadah A, Al-Qahtani M and Al-Ahwal M: Overexpression of PAK-1 is an independent predictor of disease recurrence in colorectal carcinoma. Int J Clin Exp Pathol 8: 15895-15902, 2015.
8. Goc A, Abdalla M, Al-Azayzih A and Somanath PR: Rac1 activation driven by 14-3-3ζ dimerization promotes prostate cancer cell-matrix interactions, motility and transendothelial migration. PLoS One 7: e40594, 2012.

9. Goc A, Al-Azayzih A, Abdalla M, Al-Husein B, Kavuri S, Lee J, Moses K and Somanath PR: P21 activated kinase-1 (Pak1) promotes prostate tumor growth and microinvasion via inhibition of transforming growth factor β expression and enhanced matrix metalloproteinase 9 secretion. J Biol Chem 288: 3025-3035, 2013.
10. Kichina JV, Goc A, Al-Husein B, Somanath PR and Kandel ES: PAK1 as a therapeutic target. Expert Opin Ther Targets 14: 703-725, 2010.
11. Park J, Kim JM, Park JK, Huang S, Kwak SY, Ryu KA, Kong G, Park J and Koo BS: Association of p21-activated kinase-1 activity with aggressive tumor behavior and poor prognosis of head and neck cancer. Head Neck 37: 953-963, 2015.
12. Najahi-Missaoui W, Quach ND, Jenkins A, Dabke I, Somanath PR and Cummings BS: Effect of P21-activated kinase 1 (PAK-1) inhibition on cancer cell growth, migration, and invasion. Pharmacol Res Perspect 7: e00518, 2019.
13. Verma A, Artham S, Alwhaibi A, Adil MS, Cummings BS and Somanath PR: PAK1 inhibitor IPA-3 mitigates metastatic prostate cancer-induced bone remodeling. Biochem Pharmacol 177: 113943, 2020.
14. Ong CC, Gierke S, Pitt C, Sagolla M, Cheng CK, Zhou W, Jubb AM, Strickland L, Schmidt M, Duron SG, *et al*: Small molecule inhibition of group I p21-activated kinases in breast cancer induces apoptosis and potentiates the activity of microtubule stabilizing agents. Breast Cancer Res 17: 59, 2015.
15. Deacon SW, Beeser A, Fukui JA, Rennefahrt UE, Myers C, Chernoff J and Peterson JR: An isoform-selective, small-molecule inhibitor targets the autoregulatory mechanism of p21-activated kinase. Chem Biol 15: 322-331, 2008.
16. Al-Azayzih A, Missaoui WN, Cummings BS and Somanath PR: Liposome-mediated delivery of the p21 activated kinase-1 (PAK-1) inhibitor IPA-3 limits prostate tumor growth in vivo. Nanomedicine 12: 1231-1239, 2016.
17. Quach ND, Mock JN, Scholpa NE, Eggert MW, Payré C, Lambeau G, Arnold RD and Cummings BS: Role of the phospholipase A_2 receptor in liposome drug delivery in prostate cancer cells. Mol Pharm 11: 3443-3451, 2014.
18. Adamina M, Bolli M, Albo F, Cavazza A, Zajac P, Padovan E, Schumacher R, Reschner A, Feder C, Marti WR, *et al*: Encapsulation into sterically stabilised liposomes enhances the immunogenicity of melanoma-associated Melan-A/MART-1 epitopes. Br J Cancer 90: 263-269, 2004.
19. Mock JN, Costyn LJ, Wilding SL, Arnold RD and Cummings BS: Evidence for distinct mechanisms of uptake and antitumor activity of secretory phospholipase A_2 responsive liposome in prostate cancer. Integr Biol (Camb) 5: 172-182, 2013.
20. Woodle MC and Lasic DD: Sterically stabilized liposomes. Biochim Biophys Acta 1113: 171-199, 1992.
21. Zhou R, Mazurchuk R and Straubinger RM: Antivasculature effects of doxorubicin-containing liposomes in an intracranial rat brain tumor model. Cancer Res 62: 2561-2566, 2002.
22. Zhu G, Mock JN, Aljuffali I, Cummings BS and Arnold RD: Secretory phospholipase A_2 responsive liposomes. J Pharm Sci 100: 3146-3159, 2011.
23. Fenske DB and Cullis PR: Liposomal nanomedicines. Expert Opin Drug Deliv 5: 25-44, 2008.
24. Sakakibara T, Chen FA, Kida H, Kunieda K, Cuenca RE, Martin FJ and Bankert RB: Doxorubicin encapsulated in sterically stabilized liposomes is superior to free drug or drug-containing conventional liposomes at suppressing growth and metastases of human lung tumor xenografts. Cancer Res 56: 3743-3746, 1996.
25. Maruyama K: Intracellular targeting delivery of liposomal drugs to solid tumors based on EPR effects. Adv Drug Deliv Rev 63: 161-169, 2011.
26. Fang J, Nakamura H and Maeda H: The EPR effect: Unique features of tumor blood vessels for drug delivery, factors involved, and limitations and augmentation of the effect. Adv Drug Deliv Rev 63: 136-151, 2011.
27. Deshpande PP, Biswas S and Torchilin VP: Current trends in the use of liposomes for tumor targeting. Nanomedicine (Lond) 8: 1509-1528, 2013.
28. Sawant RR and Torchilin VP: Challenges in development of targeted liposomal therapeutics. AAPS J 14: 303-315, 2012.
29. Shuler TE, Riddle CD Jr and Potts DW: Polymicrobic septic arthritis caused by *Kingella kingae* and enterococcus. Orthopedics 13: 254-256, 1990.
30. Yamashita S, Ogawa M, Sakamoto K, Abe T, Arakawa H and Yamashita J: Elevation of serum group II phospholipase A_2 levels in patients with advanced cancer. Clin Chim Acta 228: 91-99, 1994.
31. Dong Q, Patel M, Scott KF, Graham GG, Russell PJ and Sved P: Oncogenic action of phospholipase A_2 in prostate cancer. Cancer Lett 240: 9-16, 2006.
32. Belinsky GS, Rajan TV, Saria EA, Giardina C and Rosenberg DW: Expression of secretory phospholipase A_2 in colon tumor cells potentiates tumor growth. Mol Carcinog 46: 106-116, 2007.
33. Wang M, Hao FY, Wang JG and Xiao W: Group IIa secretory phospholipase A_2 (sPLA_2IIa) and progression in patients with lung cancer. Eur Rev Med Pharmacol Sci 18: 2648-2654, 2014.
34. Yamashita S, Yamashita J and Ogawa M: Overexpression of group II phospholipase A_2 in human breast cancer tissues is closely associated with their malignant potency. Br J Cancer 69: 1166-1170, 1994.
35. Zhang C, Yu H, Xu H and Yang L: Expression of secreted phospholipase A_2-Group IIA correlates with prognosis of gastric adenocarcinoma. Oncol Lett 10: 3050-3058, 2015.
36. Quach ND, Arnold RD and Cummings BS: Secretory phospholipase A_2 enzymes as pharmacological targets for treatment of disease. Biochem Pharmacol 90: 338-348, 2014.
37. Dong Z, Liu Y, Scott KF, Levin L, Gaitonde K, Bracken RB, Burke B, Zhai QJ, Wang J, Oleksowicz L and Lu S: Secretory phospholipase A_2-IIa is involved in prostate cancer progression and may potentially serve as a biomarker for prostate cancer. Carcinogenesis 31: 1948-1955, 2010.
38. Jiang J, Neubauer BL, Graff JR, Chedid M, Thomas JE, Roehm NW, Zhang S, Eckert GJ, Koch MO, Eble JN and Cheng L: Expression of group IIA secretory phospholipase A_2 is elevated in prostatic intraepithelial neoplasia and adenocarcinoma. Am J Pathol 160: 667-671, 2002.
39. Lu S and Dong Z: Overexpression of secretory phospholipase A_2-IIa supports cancer stem cell phenotype via HER/ERBB-elicited signaling in lung and prostate cancer cells. Int J Oncol 50: 2113-2122, 2017.
40. Kilkenny C, Browne W, Cuthill IC, Emerson M and Altman DG; NC3Rs Reporting Guidelines Working Group: Animal research: Reporting in vivo experiments: The ARRIVE guidelines. Br J Pharmacol 160: 1577-1579, 2010.
41. Gao F, Alwhaibi A, Sabbineni H, Verma A, Eldahshan W and Somanath PR: Suppression of Akt1-β-catenin pathway in advanced prostate cancer promotes TGFβ1-mediated epithelial to mesenchymal transition and metastasis. Cancer Lett 402: 177-189, 2017.
42. Sonnenburg DW and Morgans AK: Emerging therapies in metastatic prostate cancer. Curr Oncol Rep 20: 46, 2018.
43. Teo MY, Rathkopf DE and Kantoff P: Treatment of advanced prostate cancer. Annu Rev Med 70: 479-499, 2019.
44. Semenova G and Chernoff J: Targeting PAK1. Biochem Soc Trans 45: 79-88, 2017.
45. Rudolph J, Crawford JJ, Hoeflich KP and Wang W: Inhibitors of p21-activated kinases (PAKs). J Med Chem 58: 111-129, 2015.
46. Ndubaku CO, Crawford JJ, Drobnick J, Aliagas I, Campbell D, Dong P, Dornan LM, Duron S, Epler J, Gazzard L,*et al*: Design of Selective PAK1 Inhibitor G-5555: Improving Properties by Employing an Unorthodox Low-pK a Polar Moiety. ACS Med Chem Lett 6: 1241-1246, 2015.
47. Maksimoska J, Feng L, Harms K, Yi C, Kissil J, Marmorstein R and Meggers E: Targeting large kinase active site with rigid, bulky octahedral ruthenium complexes. J Am Chem Soc 130: 15764-15765, 2008.
48. Murray BW, Guo C, Piraino J, Westwick JK, Zhang C, Lamerdin J, Dagostino E, Knighton D, Loi CM, Zager M, *et al*: Small-molecule p21-activated kinase inhibitor PF-3758309 is a potent inhibitor of oncogenic signaling and tumor growth. Proc Natl Acad Sci USA 107: 9446-9451, 2010.
49. McCoull W, Hennessy EJ, Blades K, Chuaqui C, Dowling JE, Ferguson AD, Goldberg FW, Howe N, Jones CR, Kemmitt PD, *et al*: Optimization of highly kinase selective bis-anilino pyrimidine PAK1 Inhibitors. ACS Med Chem Lett 7: 1118-1123, 2016.
50. Shao YG, Ning K and Li F: Group II p21-activated kinases as therapeutic targets in gastrointestinal cancer. World J Gastroenterol 22: 1224-1235, 2016.
51. Karpov AS, Amiri P, Bellamacina C, Bellance MH, Breitenstein W, Daniel D, Denay R, Fabbro D, Fernandez C, Galuba I, *et al*: Optimization of a dibenzodiazepine hit to a potent and selective allosteric PAK1 inhibitor. ACS Med Chem Lett 6: 776-781, 2015.
52. Hu Q, Shang L, Wang M, Tu K, Hu M, Yu Y, Xu M, Kong L, Guo Y and Zhang Z: Co-Delivery of paclitaxel and interleukin-12 regulating tumor microenvironment for cancer immunochemotherapy. Adv Healthc Mater 9: 1901858, 2020.

53. Unal O, Akkoc Y, Kocak M, Nalbat E, Dogan-Ekici AI, Yagci Acar H and Gozuacik D: Treatment of breast cancer with autophagy inhibitory microRNAs carried by AGO2-conjugated nanoparticles. J Nanobiotechnology 18: 65, 2020.
54. Zhao H, Mu X, Zhang X and You Q: Lung cancer inhibition by betulinic acid nanoparticles via adenosine 5'-Triphosphate (ATP)-binding cassette transporter G1 gene downregulation. Med Sci Monit 26: e922092, 2020.
55. Azimee S, Rahmati M, Fahimi H and Moosavi MA: TiO2 nanoparticles enhance the chemotherapeutic effects of 5-fluorouracil in human AGS gastric cancer cells via autophagy blockade. Life Sci 248: 117466, 2020.
56. Tan L, Han S, Ding S, Xiao W, Ding Y, Qian L, Wang C and Gong W: Chitosan nanoparticle-based delivery of fused NKG2D-IL-21 gene suppresses colon cancer growth in mice. Int J Nanomedicine 12: 3095-3107, 2017.
57. Ma W, Wang X, Wang C, Gong M and Ren P: Up-regulation of P21-activated kinase 1 in osteoarthritis chondrocytes is responsible for osteoarthritic cartilage destruction. Biosci Rep 40: BSR20191017, 2020.
58. Ohori S, Mitsuhashi S, Ben-Haim R, Heyman E, Sengoku T, Ogata K and Matsumoto N: A novel PAK1 variant causative of neurodevelopmental disorder with postnatal macrocephaly. J Hum Genet 65: 481-485, 2020.
59. Horn S, Au M, Basel-Salmon L, Bayrak-Toydemir P, Chapin A, Cohen L, Elting MW, Graham JM, Gonzaga-Jauregui C, Konen O, *et al*: De novo variants in PAK1 lead to intellectual disability with macrocephaly and seizures. Brain 142: 3351-3359, 2019.
60. Kernohan KD, McBride A, Hartley T, Rojas SK; Care4Rare Canada Consortium, Dyment DA, Boycott KM and Dyack S: p21 protein-activated kinase 1 is associated with severe regressive autism, and epilepsy. Clin Genet 96: 449-455, 2019.
61. Zynda ER, Maloy MH and Kandel ES: The role of PAK1 in the sensitivity of kidney epithelial cells to ischemia-like conditions. Cell Cycle 18: 596-604, 2019.